

## Palladium Nanoparticles Encapsulated in $[M(C_{19}H_{11}N_2O_2)_2 \cdot H_2O]$ (M = Co and Mn) as a Potential Catalyst for the Homo Coupling of Aryl Halides

Ajay Kumar Jana, Raghunandan Hota, and Srinivasan Natarajan

*Cryst. Growth Des.*, **Just Accepted Manuscript** • DOI: 10.1021/acs.cgd.6b01211 • Publication Date (Web): 14 Oct 2016

Downloaded from <http://pubs.acs.org> on October 18, 2016

### Just Accepted

“Just Accepted” manuscripts have been peer-reviewed and accepted for publication. They are posted online prior to technical editing, formatting for publication and author proofing. The American Chemical Society provides “Just Accepted” as a free service to the research community to expedite the dissemination of scientific material as soon as possible after acceptance. “Just Accepted” manuscripts appear in full in PDF format accompanied by an HTML abstract. “Just Accepted” manuscripts have been fully peer reviewed, but should not be considered the official version of record. They are accessible to all readers and citable by the Digital Object Identifier (DOI®). “Just Accepted” is an optional service offered to authors. Therefore, the “Just Accepted” Web site may not include all articles that will be published in the journal. After a manuscript is technically edited and formatted, it will be removed from the “Just Accepted” Web site and published as an ASAP article. Note that technical editing may introduce minor changes to the manuscript text and/or graphics which could affect content, and all legal disclaimers and ethical guidelines that apply to the journal pertain. ACS cannot be held responsible for errors or consequences arising from the use of information contained in these “Just Accepted” manuscripts.



1  
2  
3  
4 **Palladium Nanoparticles Encapsulated in  $[M(C_{19}H_{11}N_2O_2)_2 \cdot H_2O]$  (M = Co and**  
5  
6 **Mn) as a Potential Catalyst for the Homo Coupling of Aryl Halides**  
7  
8

9  
10  
11  
12 Ajay Kumar Jana, Raghunandan Hota and Srinivasan Natarajan\*  
13

14  
15  
16  
17  
18 Framework solids Laboratory, Solid State and Structural Chemistry Unit, Indian Institute of Science,  
19  
20 Bangalore-560012, India.  
21  
22  
23  
24  
25  
26  
27  
28  
29  
30  
31  
32  
33  
34  
35  
36  
37  
38  
39  
40  
41  
42  
43  
44  
45  
46  
47  
48  
49  
50  
51  
52  
53  
54  
55

---

56  
57 \* Corresponding Author, E-mail: [snatarajan@sscu.iisc.ernet.in](mailto:snatarajan@sscu.iisc.ernet.in)  
58  
59  
60

**ABSTRACT:**

1  
2  
3  
4  
5  
6  
7  
8  
9  
10  
11  
12  
13  
14  
15  
16  
17  
18  
19  
20  
21  
22  
23  
24  
25  
26  
27  
28  
29  
30  
31  
32  
33  
34  
35  
36  
37  
38  
39  
40  
41  
42  
43  
44  
45  
46  
47  
48  
49  
50  
51  
52  
53  
54  
55  
56  
57  
58  
59  
60

A new ligand, 4-(1,10-phenanthroline-6-yl)benzoic acid, has been synthesized and employed to prepare new inorganic coordination polymer compounds,  $[M(C_{19}H_{11}N_2O_2)_2 \cdot H_2O]$  ( $M = Co, Mn$ ). Both the compounds have identical structure formed by the connectivity between octahedral metal centers and the ligand giving rise to a two-dimensional structure. The 2D structure is inter-penetrated by identical unit and forms a 2-fold interpenetrated structure. The lattice water molecules can be reversibly removed without altering the gross framework structure. The water removal has been investigated using *in-situ* IR, PXRD and *in-situ* single crystal XRD studies. Pd nanoparticles, prepared employing known procedures, were incorporated within the compound. We have successfully encapsulated up to 6.8 % of Pd with particle size of  $4.8 \pm 0.3$  nm in the compound. The Pd@MOF compound was examined for homocoupling of aryl halides, resulting in good yields and recyclability. Magnetic studies indicate anti-ferromagnetic behavior in both the compounds with good orbital contribution for the cobalt compound.

## INTRODUCTION

Heterogeneous catalysis based on noble metals such as Au, Pt, Pd as well as bimetallics such as Pt-Re, Pt-Ir and Pt-Rh have been generating continuing interest for over a century.<sup>1,2</sup> The use of noble metal nanoparticles as a catalyst was demonstrated in early 18<sup>th</sup> century by Dobereiner for the catalyzed production of water over Pt catalyst. The usefulness of the size and shape of the nanoparticles has been a topic of much discussion in recent years.<sup>3,4</sup> The nanoparticles grown in zeolites, mesoporous silica and other related porous supports underlines the importance as well as the catalytic activity, presumably due to their size confinement effects.<sup>5,6</sup> The research on strong metal supported catalyst employing metal oxides and noble metals continue to be intriguing due to their excellent performance in oil refining, auto-exhaust and other related areas. Studies on noble metal loaded graphene, graphene oxides and other similar compounds provide much hope due to their performance as efficient catalysts.<sup>7</sup> Another area that is attracting much attention is in exploiting the porous nature of the metal-organic frameworks (MOFs). These compounds possess considerable surface area as well as many chemical functionalities originating both from the organic linker as well as the metal centers, which could be beneficially harvested for useful purposes. In addition, the functional groups (associated with the organic linkers) could be exploited for the encapsulation of metal nanoparticles within the pores of the MOFs. A strategy similar to this has been exploited recently.<sup>8</sup> Noble metal nanoparticles within MOFs have been investigated before, both for enhancing the gas sorption (especially hydrogen) as well as for catalysis.<sup>9</sup> The  $\pi\cdots\pi$  interactions, present in some MOFs, have also been successfully employed for stabilizing the metal nanoparticles.

Pd-nanoparticles stabilized on MOFs have been examined as a possible route to enhance the hydrogen storage capacity.<sup>10</sup> Recent studies include the usefulness of Pd-nanoparticles as a catalyst in the C-C bond formation.<sup>11</sup> We have been interested in the study of nanoparticles assisted catalysis using MOFs. As part of this study, we have now prepared a new ligand based on 1,10-phenanthroline, 4-(1,10-phenanthroline-6-yl)benzoic acid (Scheme 1.). This ligand on reaction with cobalt and manganese yielded two new iso-structural compounds,  $[M(C_{19}H_{11}N_2O_2)_2 \cdot H_2O]$ , (M = Co, Mn). We have incorporated Pd-

1  
2  
3 nanoparticles on this compound following a previously reported procedure.<sup>12</sup> In this paper, we describe  
4 the synthesis, structure, dehydration-rehydration studies and Pd-nanoparticle assisted C–C bond  
5 formation through Suzuki coupling.  
6  
7  
8  
9

## 10 11 12 **EXPERIMENTAL SECTION**

### 13 14 **Materials**

15  
16  
17 The chemicals, 1,10-phenanthroline, oleum(15%), bromine, NH<sub>4</sub>OH, THF, CHCl<sub>3</sub>, CH<sub>2</sub>Cl<sub>2</sub>, N,N-  
18 dimethylformamide, 1,4-dioxane, potassium carbonate, sodium hydroxide, sulphuric acid, hydrochloric  
19 acid, Co(NO<sub>3</sub>)<sub>2</sub>.6H<sub>2</sub>O, MnCl<sub>2</sub>.4H<sub>2</sub>O were purchased from SDFine (India). 4-cyanophenylboronic acid,  
20 Tetrakis(triphenylphosphine) palladium(0) were acquired from Sigma–Aldrich. All the chemicals were  
21 used without further purification.  
22  
23  
24  
25  
26  
27

### 28 29 **Synthesis**

30  
31 To prepare the ligand used for the synthesis of the present compounds, we needed to prepare 5-Bromo-  
32 1,10-phenanthroline followed by 4-(1,10-phenanthrolin-6-yl)benzotrile. The initial compound 5-Bromo-  
33 1,10-phenanthroline was prepared employing a reported procedure (ESI).<sup>13</sup>  
34  
35  
36  
37

38  
39 **Synthesis of 4-(1,10-phenanthrolin-6-yl)benzoic acid:** The acid, 4-(1,10-phenanthrolin-6-yl)benzoic  
40 acid, was prepared from the nitrile compound, 4-(1,10-phenanthrolin-6-yl)benzotrile. Thus, 0.1 g (0.35  
41 mmol) 4-(1,10-phenanthrolin-6-yl)benzotrile was taken in a 100mL round bottom flask, then 20 mL 6M  
42 H<sub>2</sub>SO<sub>4</sub> solution was added and refluxed at 120 °C for 12h. The reaction mixture was cooled to room  
43 temperature and 50 mL of ice cold water was added to the reaction mixture. The resulting solid was  
44 filtered and washed with water and dried under vacuum. Yield: 0.105 g (98%). <sup>1</sup>H NMR (DMSO-d<sub>6</sub>): δ  
45 9.23(t, 2H, *J* = 4.0 Hz, *J* = 4.0 Hz), 8.80(d, 1H, *J* = 8.0 Hz), 8.44(d, 1H, *J* = 8.0 Hz), 8.18(d, 2H, *J* = 4.0  
46 Hz), 8.16(s, 1H), 8.02(q, 1H, *J* = 4.0 Hz, *J* = 4.0 Hz, *J* = 4.0 Hz), 7.93(q, 1H, *J* = 4.0 Hz, *J* = 4.0 Hz, *J* =  
47 4.0 Hz), 7.75(d, 2H, *J* = 8.0 Hz).  
48  
49  
50  
51  
52  
53  
54  
55  
56  
57  
58  
59  
60

1  
2  
3 **Synthesis of  $[M(C_{19}H_{11}N_2O_2)_2 \cdot H_2O]$  (M = Co, Mn):** For the preparation of the cobalt compound; a  
4 mixture of  $Co(NO_3)_2 \cdot 6H_2O$  (97.2 mg, 0.334 mmol), 4-(1,10-phenanthroline-6-yl)benzoic acid (50 mg,  
5 0.167 mmol), N,N-dimethylformamide (4 mL), ethanol (4 mL), and water (4 mL) was taken in a 23 mL  
6 Teflon-lined autoclave and heated at 150°C for 3 days. The resulting product contained red colored rod  
7 like crystals, which were filtered, washed with water and ethanol and dried in vacuum. Yield: 42.9 mg  
8 (38%). Elemental analysis (%) for  $[Co(C_{19}H_{11}N_2O_2)_2 \cdot H_2O]$  Found (Calculated): C 67.01 (67.56), H 3.39  
9 (3.58), N 8.28 (8.29). A similar procedure was followed for the preparation of the Mn analogue by using  
10  $MnCl_2 \cdot 4H_2O$  and heating the reaction mixture at 120°C for 3 days. Yield: 26.9 mg (24%). Elemental  
11 analysis (%) for  $[Mn(C_{19}H_{11}N_2O_2)_2 \cdot H_2O]$  Found (Calculated): C 67.61 (67.96), H 3.38 (3.60), N 8.18  
12 (8.34).  
13  
14  
15  
16  
17  
18  
19  
20  
21  
22  
23  
24  
25

26 **Initial Characterization and Physical Measurements:** The ligand was characterized employing NMR  
27 spectroscopy.  $^1H$  NMR data were collected using Bruker 400 MHz spectrometer. Chemical shifts are  
28 reported in ppm using tetramethylsilane as the internal reference (Supporting Information, Figure S1-S3).  
29 IR spectra were recorded as KBr pellets using a FTIR spectrometer (Perkin Elmer, model no: L125000P).  
30 UV-Vis spectra were recorded at room temperature (Perkin Elmer Lambda 35 spectrophotometer)  
31 (Supporting Information, Figure S4). Room temperature solid state photoluminescence studies were  
32 carried out on the compounds (Perkin Elmer LS 55 luminescence spectrophotometer) (Supporting  
33 Information, Figure S5). Elemental analyses (carbon, hydrogen, and nitrogen) were performed in a  
34 Thermo Finnigan EA Flash 1112 Series. Thermogravimetric analysis (TGA) (Metler-Toledo) was carried  
35 out in oxygen atmosphere (flow rate = 40 mL/min) in the temperature range 30–800°C (heating rate =  
36 10°C / min) (Supporting Information, Figure S6). Powder X-ray diffraction (XRD) patterns were  
37 recorded in the  $2\theta$  range 5–50° using  $Cu K\alpha$  radiation (Philips X'pert). Magnetic studies were carried out  
38 in the temperature range of 2–300 K using a SQUID magnetometer (Quantum Design, USA). ICP-OES  
39 study was performed using Perkin Elmer Optima 2000DV spectrometer. Transmission electron  
40 microscopy (TEM), high resolution TEM (HRTEM) images and energy-dispersive X-ray spectroscopy  
41  
42  
43  
44  
45  
46  
47  
48  
49  
50  
51  
52  
53  
54  
55  
56  
57  
58  
59  
60

(EDS) were obtained with a JEM 2100F, JEOL transmission electron microscope at an accelerating voltage of 200 kV.

**Single-Crystal Structure Determination:** Suitable single crystals were carefully selected under a polarizing microscope and glued to a glass fiber. Single crystal data were collected at room temperature and at 475 K on an Oxford Xcalibur (Mova) diffractometer equipped with an EOS CCD detector. The X-ray generator was operated at 50 kV and 0.8 mA using Mo  $K_{\alpha}$  ( $\lambda = 0.71073 \text{ \AA}$ ) radiation. The cell refinement and data reduction were accomplished using CrysAlis RED.<sup>14</sup> The structure was solved by direct methods and refined using SHELX97 present in the WinGX suit of programs (version 1.63.04a).<sup>15</sup> The hydrogen positions were located initially from the difference Fourier maps and for the final refinement, the hydrogen positions were fixed in a geometrically ideal position and refined employing a riding model. The final refinements included the atomic positions for all the atoms, anisotropic thermal parameters for all the non-hydrogen atoms, and isotropic thermal parameters for all the hydrogen atoms. The details of the structure solution and final refinement parameters are given in Table 1. The CCDC numbers for the compounds **1**, **2**, **1a** and **2a** are 1496623, 1497203, 1497207 and 1497209 respectively. These data can be obtained free of charge from The Cambridge Crystallographic Data Center (CCDC) via [www.ccdc.cam.ac.uk/data\\_request/cif](http://www.ccdc.cam.ac.uk/data_request/cif).

**Synthesis of Pd@MOF:** Pd nanoparticles loaded on the compounds were carried out by following a reported procedure (ESI).<sup>12</sup>

**Pd@MOF characterization:** The Pd loaded compounds were characterized by IR, ICP-OES analysis and electron-microscopic technique. Structurally, one of the carboxylate oxygen is found to be free and available for chemical manipulation. From the infrared spectroscopic analysis, we find that the Pd loaded compound exhibits a shift in the carbonyl stretching frequency. We observed a shift of  $\sim 6 \text{ cm}^{-1}$  between the as synthesized compound and the Pd-containing one ( $1607 \text{ cm}^{-1}$  for the compound and  $1601 \text{ cm}^{-1}$  for the Pd@MOF) (Figure 1). Similar shifting of the IR frequency has also been noted earlier for the Pd-

1  
2  
3 loaded compounds.<sup>16</sup> This suggests that the Pd nanoparticles would be distributed evenly across the  
4 compound. The shift in the carbonyl frequency could be due to the partial electron donation from the  
5 carbonyl group to the Pd-Nanoparticles, which would lead to a weakening of the carbonyl bond.<sup>17</sup> The  
6 inductively coupled plasma optical emission spectrometry (ICP-OES) analysis on the Pd-loaded  
7 compound gave a Pd-loading of 6.8 wt%, which is also reasonably high. The transmission electron  
8 microscopic (TEM) investigation on the Pd-loaded compound also suggests that the particles are evenly  
9 distributed with particle sizes in the range of  $4.8 \pm 0.3$  nm (Figure 2). The HRTEM studies on the  
10 nanoparticles clearly indicated a lattice spacing of 0.23 nm, which would correspond to the [111] plane of  
11 the *fcc* structure of the Pd. XPS analysis was carried out on the Pd-loaded samples, which clearly  
12 indicated the presence of Pd<sup>0</sup> state (Figure 3).  
13  
14  
15  
16  
17  
18  
19  
20  
21  
22  
23  
24  
25  
26  
27

28 **Thermogravimetric Analysis:** The thermogravimetric studies on cobalt compound indicated a small  
29 weight loss in the temperature range 30-210°C followed by a sharp drop at ~380°C (Supporting  
30 Information, Figure S6). The initial weight of ~ 2.5% corresponds to the loss of one lattice water  
31 molecule (cal. 2.6%). The second weight loss at ~380°C of ~ 81% corresponds to the loss of the ligand  
32 (cal. 88.5%). The final calcined product was found to be crystalline by PXRD and can be identified as  
33 Co<sub>3</sub>O<sub>4</sub> (JCPDS: 43-1003). A similar behavior was also observed for the manganese compound  
34 (Supporting Information, Figure S6). The decomposition product was found to be a mixture of Mn<sub>3</sub>O<sub>4</sub>  
35 (JCPDS: 89-4837) and Mn<sub>2</sub>O<sub>3</sub> (JCPDS: 89-4836). The loss of lattice water molecule from the structure  
36 was also established employing *in-situ* IR spectroscopic studies. From the *in-situ* IR spectroscopic  
37 studies, we observed that the O-H stretching bands ( $3466\text{ cm}^{-1}$  for Co and  $3420\text{ cm}^{-1}$  for Mn) of the lattice  
38 water molecule disappear as the temperature is raised from RT to 220°C (Figure 4). This indicates that the  
39 water molecules can be removed in a facile manner from the structure. The PXRD studies on the  
40 dehydrated sample also indicated that the samples are crystalline and comparable to the as synthesized  
41 compound (Supporting Information, Figure S8). This suggested the possibility of obtaining single crystal  
42  
43  
44  
45  
46  
47  
48  
49  
50  
51  
52  
53  
54  
55  
56  
57  
58  
59  
60



1  
2  
3 structure on the dehydrated compound. To this end, we attempted an *in-situ* study on the single crystal  
4  
5 and we did obtain the dehydrated structure (described below).  
6  
7

## 8 RESULTS AND DISCUSSION 9

10  
11 **Structure of  $[M(C_{19}H_{11}N_2O_2)_2 \cdot H_2O]$ , (M = Co and Mn):** The asymmetric unit consists of 25 non  
12  
13 hydrogen atoms. The metal ions, occupying a special position with a site multiplicity of 0.5, are  
14  
15 octahedrally coordinated with two oxygen {O2(#1), O2(#2)} and four nitrogen {N1, N2, N1(#3), N2(#3)}  
16  
17 atoms (Figure 5). The average M–O and M–N bond lengths are 2.014Å, 2.166Å for Co and 2.026Å,  
18  
19 2.186Å for Mn (Supporting Information, Table S1). The ligand, 4-(1,10-phenanthroline-6-yl)benzoic acid,  
20  
21 connects with both the phenanthroline nitrogen as well as through the carboxylate oxygen with the metal  
22  
23 ions. Thus, the ligands links two metal centers, which gives rise to a two-dimensional layer arrangement  
24  
25 (Figure 6). The large size of the ligand separates the metal ions apart and results in the formation of  
26  
27 rhombus grid with an interior angle of 93.76° and 86.24°. The large opening within the layers allows  
28  
29 another two dimensional layer to be interpenetrated at an angle of 65.86° (Figure 7) and results in the  
30  
31 formation of a two-fold interpenetrated structure (Figure 8). The two dimensional layers are further  
32  
33 hydrogen bonded with its adjacent layers (Supporting Information, Figure S11) through the lattice water  
34  
35 (O3) molecule present in the crystal structure, with O3···O1 distances of 2.823(3)Å–2.836(3)Å and O3–  
36  
37 H3A···O1 angles of 168(3)°–172(3)° (Supporting Information, Table S2). This lattice water molecule  
38  
39 also occupies a special position with site multiplicity of 0.5. Apart from the hydrogen bonding involving  
40  
41 lattice water molecule, C–H···O interactions with C1–H1···O1, C4–H4···O3 are also observed in the  
42  
43 structure (Supporting Information, Figure S12, Table S2). In addition, we have also observed C–H··· $\pi$   
44  
45 interactions as well.  
46  
47  
48  
49  
50  
51  
52

53 The dehydrated structures of the compounds have exactly the same connectivity with respect to  
54  
55 the metal ion and the carboxylates. The absence of lattice water (O3) molecule in the structure resulted in  
56  
57 minor modifications in the lattice parameters as well as the cell volume (Table 1). In addition, the inter  
58  
59  
60

1  
2  
3 layer hydrogen bonding (O3–H3A···O1) as well as the C4–H4···O3 hydrogen bonding was absent. The  
4  
5 other interactions observed in the parent compound were also observed in the dehydrated compounds  
6  
7 (Supporting Information, Table S2).  
8  
9

10  
11 **Optical studies:** The UV-Vis spectra of the ligand (Supporting Information, Figure S4) indicated  
12  
13 absorptions corresponding to  $\pi$ - $\pi^*$  and n- $\pi^*$  transitions (see table S3, ESI). The compounds, expectedly,  
14  
15 exhibited a red shift in the absorption bands. In addition, we have been able to observe the allowed d-d  
16  
17 transitions of the central transition metal ions (Co / Mn). All the observed absorptions are listed in Table  
18  
19 S3. Similar absorptions have been observed earlier for the Co and Mn compounds.<sup>18,19</sup> The room  
20  
21 temperature photo luminescence investigations also indicated a behavior that is expected of the  
22  
23 compounds and the ligand (ESI, Figure S5 and Table S3). As a case study, we have also carried out the  
24  
25 UV-Vis spectroscopic analysis of the palladium loaded cobalt compound (ESI, Figure S4d), which did  
26  
27 not exhibit any changes in the 200 – 350nm region. After 350nm, the absorbance of the palladium loaded  
28  
29 compound was found to increase gradually, which may be due to the surface plasmon absorption of the  
30  
31 Pd nanoparticles. Similar observations have been made earlier.<sup>20</sup>  
32  
33  
34  
35  
36  
37  
38

39 **Infrared (IR) spectroscopic studies:** Infrared (IR) spectroscopic studies were carried out in the mid-IR  
40  
41 region on KBr pellets. The IR spectra of 4-(1,10-phenanthroline-6-yl)benzotrile exhibited typical bands.  
42  
43 The band at 2227  $\text{cm}^{-1}$  corresponds to the nitrile group. After acid hydrolysis of 4-(1,10-phenanthroline-6-  
44  
45 yl)benzotrile the band at 2227 $\text{cm}^{-1}$  disappeared along with the appearance of two new bands at 1715  $\text{cm}^{-1}$   
46  
47 and 3392  $\text{cm}^{-1}$ , which clearly indicated that the nitrile group transformed to a carboxylic acid group  
48  
49 (Supporting Information, Figure S13). Other typical bands have also been observed. Important IR bands  
50  
51 have been tabulated (Supporting Information, Table S4). For the cobalt and manganese compounds, a  
52  
53 broad band in the region of  $\sim$ 3300–3500  $\text{cm}^{-1}$ , suggested the presence of water molecule (Supporting  
54  
55  
56  
57  
58  
59  
60

1  
2  
3 Information, Figure S14). Other bands typical of aromatic backbone of the ligand were also observed  
4  
5 (Supporting Information, Table S4).  
6  
7

8 **Magnetic Studies:** The magnetic behavior as a function of temperature of the cobalt and manganese  
9  
10 compounds were carried out in the temperature range 300-2K (Figure 9). For the cobalt compound, the  
11  
12 magnetic susceptibility decreases very slowly up to 25K and then increases sharply (Supporting  
13  
14 Information, Figure S15a). A similar behavior was also noted for the Mn-compound (Supporting  
15  
16 Information, Figure S15b). The room temperature, the  $\chi_m T$  (1000 Oe) values were found to be 4.767 and  
17  
18 5.841  $\text{emu mol}^{-1} \text{K}$ , respectively, for the Co and Mn compounds. For the Co-compound, the obtained  $\chi_m T$   
19  
20 value at room temperature (4.767  $\text{emu mol}^{-1} \text{K}$ ) was found to be higher than the expected spin-only value  
21  
22 of 3.873  $\text{emu mol}^{-1} \text{K}$ . This suggests a large orbital contribution to the effective magnetic moment in the  
23  
24 case of Co. Cobalt compounds exhibiting large orbital contribution is well known.<sup>21</sup> The Mn compound,  
25  
26 on the other hand, exhibits a spin-only value of 5.916  $\text{emu mol}^{-1} \text{K}$ . The  $\chi_m T$  value shows a continuous  
27  
28 decrease with decreasing temperature up to 29K to reach a value of 2.66  $\text{emu mol}^{-1} \text{K}$  for the Co-  
29  
30 compound and 3.72  $\text{emu mol}^{-1} \text{K}$  for the Mn-compound. On cooling further the  $\chi_m T$  exhibits a sharp  
31  
32 increase to reach a maximum value of 4.4  $\text{emu mol}^{-1} \text{K}$  (Co) and 4.06  $\text{emu mol}^{-1} \text{K}$  (Mn) at 25K. The  
33  
34  $\chi_m T$  values starts to decrease on cooling below 25K. The sharp increase clearly suggests the onset of long-  
35  
36 range magnetic ordering. The high temperature magnetic data was fitted to a Curie-Weiss behavior in the  
37  
38 temperature range 100-300 K, which gave a value of  $-90.2 \text{ K}$  for Co-compound and  $-61.1 \text{ K}$  for Mn-  
39  
40 compound (inset Figure 9a and 9b). The large negative values for the  $\theta_p$  suggest that the magnetic centers  
41  
42 are anti-ferromagnetically coupled. It may be noted that the metal ions ( $\text{Co}^{2+}/\text{Mn}^{2+}$ ) are separated from  
43  
44 each other by 13.397Å, but are connected by a conjugated ligand. We believe that the large negative  
45  
46 values indicates strong anti-ferromagnetic coupling between the metal centers mediated through the  
47  
48 organic linker. The M-H studies at 2K indicate a typical behavior observed for samples exhibiting anti-  
49  
50 ferromagnetic interactions. The maximum saturation magnetization values of 2.58  $\text{emu mol}^{-1}$  (Co) and  
51  
52  
53  
54  
55  
56  
57  
58  
59  
60

1  
2  
3 4.33 emu mol<sup>-1</sup> (Mn) were observed at 9T (Supporting Information, Figure S16). These values are  
4  
5 comparable to the expected saturation values of 3 (Co) and 5 (Mn) for one uncoupled Co<sup>2+</sup> and Mn<sup>2+</sup> ion.  
6  
7

8 **Suzuki coupling reaction:** The usefulness of Pd-nanoparticles encapsulated in the compound was  
9 examined by carrying out a homocoupling (C–C coupling) reaction (Suzuki coupling). Thus, Suzuki  
10 coupling reaction between iodobenzene (0.5 mmol) and phenylboronic acid (0.75 mmol) was carried out  
11 with 2 mol% of Pd@cobalt and K<sub>2</sub>CO<sub>3</sub> (1.0 mmol) at 75°C in a mixture of THF:MeOH solvent. The  
12 various experimental conditions were arrived by carrying out reactions from room temperature to 90°C  
13 (Table 2). As can be noted, the C–C coupling reaction preceded only about 15% at room temperature. The  
14 highest yield of 95.1% was achieved after 15h at 75°C. No increase in the yield was obtained at higher  
15 temperature (90°C) under the same conditions. The same reaction when carried out on pristine cobalt  
16 compound at 75°C for larger duration (24h) did not yield any additional significant progress of the  
17 reaction. Our efforts at other derivatives such as with electron donating group (-Me, -OMe) gave smaller  
18 yields of the product (Table 3). This observation appears to be consistent with those reported before.<sup>22</sup>  
19  
20 Similar experiment carried out with Pd@manganese also behaved in a similar way with the iodo  
21 derivative (Supporting Information, Figure S17). The same reaction, when carried out with bromo- and  
22 chloro- derivatives gave much reduced products with the chloro-derivatives gave yields in the range of ~  
23 12-19% (Table 3). The recyclability of the Pd-loaded catalyst was examined under the standardized  
24 conditions which gave yields of ~ 85% and ~ 76%, respectively (Figure 10). The stability of the catalyst  
25 after the coupling reactions was examined by PXRD (Supporting Information, Figure S18), which clearly  
26 indicated that the compounds retain their structures even after the 3rd cycle.  
27  
28

29  
30 We have also carried out XPS studies of the catalyst, after the reaction, to learn about the changes  
31 in the oxidation state of the Pd metal. The studies indicated again two peaks at 340.85 eV and 335.67 eV  
32 which are comparable to the as prepared sample and can be assigned to Pd(0) 3d<sub>3/2</sub> and Pd(0) 3d<sub>5/2</sub>  
33 respectively (Figure 3b). In order to probe the heterogeneous nature of the reaction, we have performed a  
34 hot filtration experiment. Thus, a mixture of iodobenzene (0.5 mmol), phenylboronic acid (0.75 mmol),  
35  
36  
37  
38  
39  
40  
41  
42  
43  
44  
45  
46  
47  
48  
49  
50  
51  
52  
53  
54  
55  
56  
57  
58  
59  
60

1  
2  
3 K<sub>2</sub>CO<sub>3</sub> (1.0 mmol), THF (2.5 mL), MeOH (0.25mL) and Pd@MOF (16 mg, 2 mol %) was reacted at  
4  
5 75°C. After 1h of the reaction, the catalyst was separated from the reaction mixture by centrifugation and  
6  
7 the filtrate was allowed to continue the reaction at 75°C. The yield of the product was analyzed. The  
8  
9 yield of the reaction with the Pd@MOF and without Pd@MOF is shown in Figure 11. It may be noted  
10  
11 that in the absence of Pd@MOF, the change in the yield was found to be ~10%. The yield actually  
12  
13 increases from 25% at 1h to 35% at 12h. This observation suggests that there is no significant progress in  
14  
15 the reaction when the filtrate, containing the reaction mixture without the catalyst, was allowed to  
16  
17 continue at the same reaction conditions for longer duration. It is likely that the filtrate might have some  
18  
19 trace residue of the catalytically active Pd metal, which gives rise to this small increase in the yield. The  
20  
21 amount of Pd content in the filtrate was analyzed by ICP-OES analysis, which indicated a Pd  
22  
23 concentration (leached) of ~1.2 ppm, which would correspond to ~5.6 % of the original Pd amount in the  
24  
25 catalyst. We have also carried out a similar experiment by doubling the concentration of all the reactants,  
26  
27 including the catalyst. The results were found to be similar and consistent to the first experiment. The  
28  
29 efficiency of the Pd@MOF was compared with other Pd nanoparticles supported catalysts (Supporting  
30  
31 Information, Table S5). It can be noted that the catalytic activity of Pd@MOF is comparable with many  
32  
33 of the reported activities. It is clear that the activity of the catalyst depends on the size of the metal  
34  
35 nanoparticles with smaller metal nanoparticles giving better catalytic activity, possibly due to the  
36  
37 availability of higher active surface area for the reactants. We believe that the higher catalytic activity  
38  
39 observed in the presence of Pd@MOF could be due to the wide dispersion of smaller Pd nanoparticles  
40  
41 over the surface of the compound investigated in the present study.  
42  
43  
44  
45

## 46 CONCLUSIONS

47  
48 A solvothermal reaction involving 4-(1,10-phenanthroline-6-yl)benzoic acid and metal salts  
49  
50 (cobalt / manganese) resulted in two compounds, [M(C<sub>19</sub>H<sub>11</sub>N<sub>2</sub>O<sub>2</sub>)<sub>2</sub>.H<sub>2</sub>O], (M = Co, Mn). Both the  
51  
52 compounds have identical structure and possess 2-fold interpenetrated framework. The extra-framework  
53  
54 water molecules have been shown to be reversibly removed by *in-situ* IR and single crystal investigations.  
55  
56 Palladium nanoparticles with 4.8 ± 0.3 nm size were successfully encapsulated in the compound. The  
57  
58  
59  
60

Pd@MOF compounds exhibits excellent catalytic properties with good recyclability for the homo-coupling of aryl halides, especially for the iodo derivatives. Magnetic studies indicate strong anti-ferromagnetic exchanges between the metal centers mediated through the aromatic linker.

## ACKNOWLEDGEMENTS

SN thanks the Science and Engineering Research Board (SERB), Government of India for the award of a research grant as well as a J. C. Bose National Fellowship. Council of Scientific and Industrial Research (CSIR), Government of India, is thanked for a research grant (S.N.) and a research fellowship (A.K.J.).

## ASSOCIATED CONTENT

### Supporting Information

The Supporting Information is available free of charge on the ACS Publications website at DOI:.

Supporting materials contain selected bond lengths and bond angles for 1–2a, intermolecular interactions present in the crystal structures, UV-Vis and photoluminescence investigations, IR bands, related reported Suzuki coupling reactions, synthesis of 5-Brphen and 4-(1,10-phenanthroline-6-yl)benzotrile. Figures of <sup>1</sup>H NMR spectra, UV–Vis absorption spectra, photoluminescence spectra, TGA, PXRD patterns, synthesis and color of Pd@MOF, EDX pattern of Pd@cobalt, size distribution of Pd nanoparticles, sample preparation procedure for ICP-OES analysis, hydrogen bonding present in the crystal structure, magnetic measurements plots, results of catalytic reactions and characterization data of the catalytic products and figures of asymmetric unit of 1–2a.

## REFERENCES:

- (1) Thomas, J. M.; *Angew. Chem. Int. Ed.* **1994**, *33*, 913.
- (2) Thomas, J. M.; *Angew. Chem. Int. Ed.* **1999**, *38*, 3588.
- (3) Cao, S.; Tao, Fr.; Tang, Y.; Li, Y.; Yu, J. *Chem. Soc. Rev.* **2016**, DOI: 10.1039/c6cs00094k.
- (4) Tanga, Y.; Cheng, W. *Nanoscale* **2015**, *7*, 16151.
- (5) Djakovitch, L.; Koehler, K. *J. Am. Chem. Soc.* **2001**, *123*, 5990.
- (6) Cai, M.; Sha, J.; Xu, Q. *J. Mol. Catal. A: Chem.* **2007**, *268*, 82.
- (7) Siamaki, A. R.; Khder, A. E. R. S.; Abdelsayed, V.; El-Shall, M. S. and Gupton, B. F. *Journal of Catalysis* **2011**, *279*, 1.
- (8) Mondal, B.; Acharyya, K.; Howlader, P.; Mukherjee, P. S. *J. Am. Chem. Soc.* **2016**, *138*, 1709.
- (9) Suh, M. P.; Park, H. J.; Prasad, T. K.; Lim, D. *Chem. Rev.* **2012**, *112*, 782.
- (10) Cheon, Y. E.; Suh, M. P. *Angew. Chem. Int. Ed.* **2009**, *48*, 2899.
- (11) Seechurn, C. C. C. J.; Kitching, M. O.; Colacot, T. J.; Snieckus, V. *Angew. Chem. Int. Ed.* **2012**, *51*, 5062.
- (12) Li, L.; Zhao, H.; Wang, J.; Wang, R. *ACS Nano* **2014**, *8*, 5352.
- (13) Hissler, M.; Connick, W. B.; Geiger, D. K.; McGarrah, J. E.; Lipa, D.; Lachicotte, R. J.; Eisenberg, R. *Inorg. Chem.* **2000**, *39*, 447.
- (14) *CrysAlis CCD, CrysAlis PRO RED*, version 1.171.33.34d; Oxford Diffraction Ltd.: Abingdon, Boxfordshire, England, 2009.
- (15) Sheldrick, G. M. *SHELXS-97, Program for Crystal Structure Solution and Refinement*, University of Göttingen, Göttingen, Germany, 1997.
- (16) Chen, L.; Chen, H.; Luque, R.; Li, Y. *Chem. Sci.* **2014**, *5*, 3708.
- (17) Nemamcha, A.; Rehspringer, J.; Khatmi, D. *J. Phys. Chem. B* **2006**, *110*, 383.
- (18) Ramaswamy, P.; Mandal, S.; Hegde, N. N.; Prabhu, R.; Banerjee, D.; Bhat, S. V.; Natarajan, S. *Eur. J. Inorg. Chem.* **2010**, 1829.

- 1  
2  
3 (19) Bhattacharya, S.; Ramanujachary, K. V.; Lofland, S. E.; Magdalenoc, T.; Natarajan, S.  
4  
5 *CrystEngComm.* **2012**, *14*, 4323.  
6  
7 (20) Leong, K. H.; Chu, H. Y.; Ibrahim, S.; Saravanan, P. *Beilstein J. Nanotechnol.* **2015**, *6*, 428.  
8  
9 (21) Vallejo, J.; Fortea-Perez, F. R.; Pardo, E.; Benmansour, S.; Castro, I.; Krzystek, J.; Armentanoc,  
10  
11 D.; Cano, J. *Chem. Sci.* **2016**, *7*, 2286.  
12  
13 (22) In'es, B.; SanMartin, R.; Moure, M. J.; Dom'inguez, E. *Adv. Synth. Catal.* **2009**, *351*, 2124.  
14  
15  
16  
17  
18  
19  
20  
21  
22  
23  
24  
25  
26  
27  
28  
29  
30  
31  
32  
33  
34  
35  
36  
37  
38  
39  
40  
41  
42  
43  
44  
45  
46  
47  
48  
49  
50  
51  
52  
53  
54  
55  
56  
57  
58  
59  
60



**Figure Captions.**

**Figure 1.** The IR spectra of the cobalt compound and the palladium loaded one. Please note the shift in the IR band (see text).

**Figure 2.** Figure shows the palladium loaded cobalt compound: (a) TEM image of Pd(0)@cobalt compound (b) HRTEM image of the palladium nanoparticles. Note the inter planar spacing of 0.224 nm corresponding to Pd (111) lattice plane.

**Figure 3.** (a) The XPS spectra of Pd loaded compound, showing the peaks corresponding to Pd (0). (b) The XPS spectra of the catalyst after the catalytic reaction, showing the peaks corresponding to Pd (0).

**Figure 4:** Variable temperature IR spectra for the compounds: (a) Cobalt (b) Manganese.

**Figure 5.** Figure shows the coordination environment around the metal ion forming the octahedral geometry (shown in the inset).

**Figure 6.** (a) Two dimensional rhombus layer observed in the cobalt and the manganese compound. (b) Schematic representation of the 2D grid (green ball represent the metal ions and the black stick represents the ligand).

**Figure 7.** Figure shows the schematic representation of the interpenetration of the 2D layer. Note that the other layer interpenetrates in an orthogonal manner.

**Figure 8.** Figure shows the interpenetration of layers.

**Figure 9.** Figure shows the thermal variation of  $\chi_m T$  for both the compounds. Inset shows the  $1/\chi_m$  vs. T (a) Co (b) Mn.

**Figure 10.** Recyclability studies for the homocoupling reaction employing Pd@cobalt compound.

1  
2  
3 **Figure 11.** Results of the hot filtration experiment for the Suzuki coupling reaction: (■ normal reaction in  
4 the presence of the catalyst ● the measured yield when the catalyst was removed by centrifugation after  
5  
6  
7  
8 1h).  
9  
10  
11  
12  
13  
14  
15  
16  
17  
18  
19  
20  
21  
22  
23  
24  
25  
26  
27  
28  
29  
30  
31  
32  
33  
34  
35  
36  
37  
38  
39  
40  
41  
42  
43  
44  
45  
46  
47  
48  
49  
50  
51  
52  
53  
54  
55  
56  
57  
58  
59  
60

Table 1. Crystal Data and Structure Refinement Parameters for 1–2a.

Structural parameter	<b>1</b>	<b>2</b>	<b>1a</b>	<b>2a</b>
Empirical formula	[Co(C <sub>19</sub> H <sub>11</sub> N <sub>2</sub> O <sub>2</sub> ) <sub>2</sub> ·H <sub>2</sub> O]	[Mn(C <sub>19</sub> H <sub>11</sub> N <sub>2</sub> O <sub>2</sub> ) <sub>2</sub> ·H <sub>2</sub> O]	[Co(C <sub>19</sub> H <sub>11</sub> N <sub>2</sub> O <sub>2</sub> ) <sub>2</sub> ]	[Mn(C <sub>19</sub> H <sub>11</sub> N <sub>2</sub> O <sub>2</sub> ) <sub>2</sub> ]
Formula weight	675.54	671.55	657.53	653.54
Crystal system	Orthorhombic	Orthorhombic	Orthorhombic	Orthorhombic
Space group	I b a 2	I b a 2	I b a 2	I b a 2
a (Å)	10.6323(5)	10.5810(5)	10.7196(10)	10.6843(10)
b (Å)	16.4151(9)	16.5660(9)	16.9591(13)	17.2404(13)
c (Å)	18.3130(10)	18.6370(10)	17.6231(15)	17.7573(15)
α (deg)	90	90	90	90
β (deg)	90	90	90	90
γ (deg)	90	90	90	90
V (Å <sup>3</sup> )	3196.2(3)	3266.8(3)	3203.8(5)	3270.9(5)
Z	4	4	4	4
T/K	298	298	475	475
ρ (calc/gcm <sup>-3</sup> )	1.404	1.365	1.363	1.327
μ (mm <sup>-1</sup> )	0.589	0.455	0.583	0.450
λ(Mo Kα/Å)	0.71073	0.71073	0.71073	0.71073
θ range (°)	3.19 – 24.99	3.16 – 25.00	3.22 – 25.00	3.21 – 25.000
R indexes [ I > 2σ (I)]	R1 = 0.0271 wR2 = 0.0590	R1 = 0.0291 wR2 = 0.0677	R1 = 0.0436 wR2 = 0.0809	R1 = 0.0485 wR2 = 0.1056
R indexes (all data)	R1 = 0.0358 wR2 = 0.0611	R1 = 0.0384 wR2 = 0.0700	R1 = 0.0630 wR2 = 0.0917	R1 = 0.0691 wR2 = 0.1215

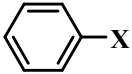
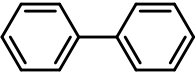
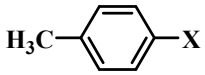
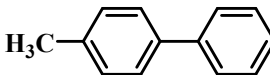
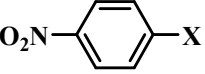
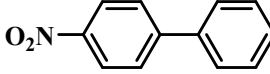
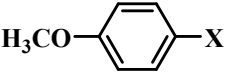
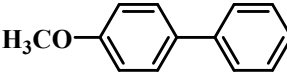
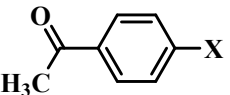
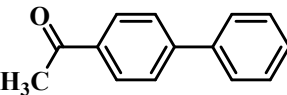
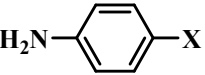
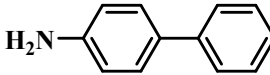
1  
2  
3  $^a R_1 = \Sigma|F_o| - |F_c|/\Sigma|F_o|$ ;  $wR_2 = \{\Sigma|w(F_o^2 - F_c^2)|/\Sigma [w(F_o^2)^2]\}^{1/2}$ .  $w = 1/[\rho^2(F_o)^2 + (aP)^2 + bP]$ .  $P = [\max$   
4  
5  $(F_o;O) + 2(F_c)^2]/3$ , where  $a = 0.0331$  and  $b = 0.4577$  for **1**,  $a = 0.0385$  and  $b = 0.4166$  for **2**,  $a = 0.0325$  and  
6  
7  
8  $b = 0.0000$  for **1a**,  $a = 0.0542$  and  $b = 0.0000$  for **2a**.  
9  
10  
11  
12  
13  
14  
15  
16  
17  
18  
19  
20  
21  
22  
23  
24  
25  
26  
27  
28  
29  
30  
31  
32  
33  
34  
35  
36  
37  
38  
39  
40  
41  
42  
43  
44  
45  
46  
47  
48  
49  
50  
51  
52  
53  
54  
55  
56  
57  
58  
59  
60

**Table 2.** Suzuki coupling reaction of iodobenzene and phenylboronic acid with and without Pd@cobalt catalysts at different temperature.

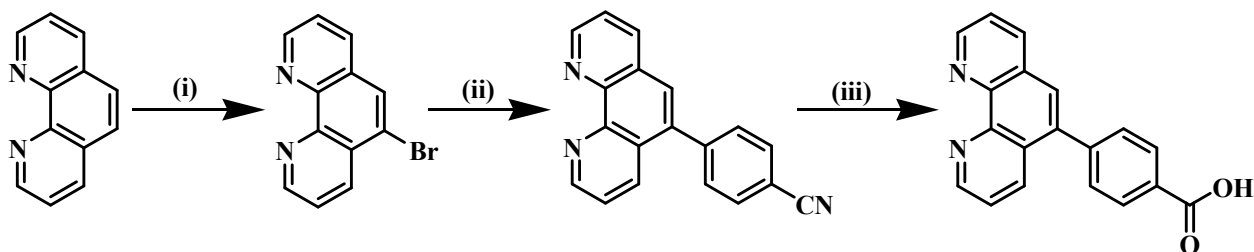
Entry	Catalyst	Temperature (°C)	Time	% Yield
1	Cobalt compound	75	24h	-
2	Pd@cobalt compound	25	24h	15
3	Pd@cobalt compound	50	24h	62
4	Pd@cobalt compound	75	15h	95.1
5	Pd@cobalt compound	90	15h	95.1

Reaction conditions: Aryl iodide (0.5 mmol), phenylboronic acid (0.75 mmol), K<sub>2</sub>CO<sub>3</sub> (1.0 mmol), THF (2.5 mL), MeOH (0.25mL) and 6.8 wt% Pd@MOF (16 mg, 2 mol% of Pd, 0.01 mmol). Yield based on column chromatography.

**Table 3.** Suzuki coupling reaction of aryl halide derivative catalyzed by Pd@cobalt compound.

S. No.	Substrate	Reaction time	Product	Yield %		
				Cl	Br	I
1		15h (X=I, Br) 24h (X=Cl)		12.8	90.5	95.1
2		15h (X=I, Br) 24h (X=Cl)		12.4	82.2	92.6
3		15h (X=I, Br) 24h (X=Cl)		18.2	91.4	96.2
4		15h (X=I, Br) 24h (X=Cl)		15.6	85.4	93.7
5		15h (X=I, Br) 24h (X=Cl)		13.5	89.5	95.1
6		15h (X=I, Br) 24h (X=Cl)		11.3	83.2	91.6

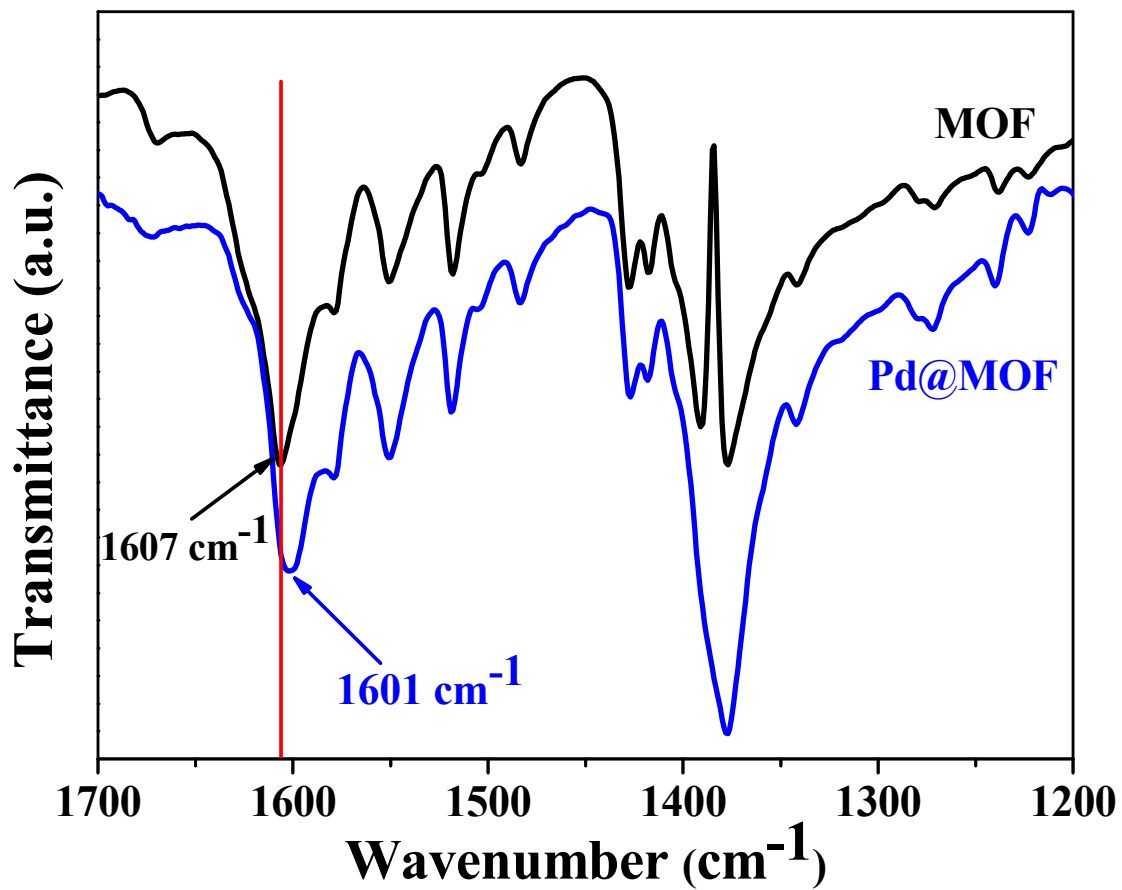
Reaction conditions: Aryl halide (0.5 mmol), phenylboronic acid (0.75 mmol),  $K_2CO_3$  (1.0 mmol), THF (2.5 mL), MeOH (0.25mL) and 6.8 wt% Pd@MOF (16 mg, 2 mol % Pd, 0.01 mmol). Yield based on column chromatography.



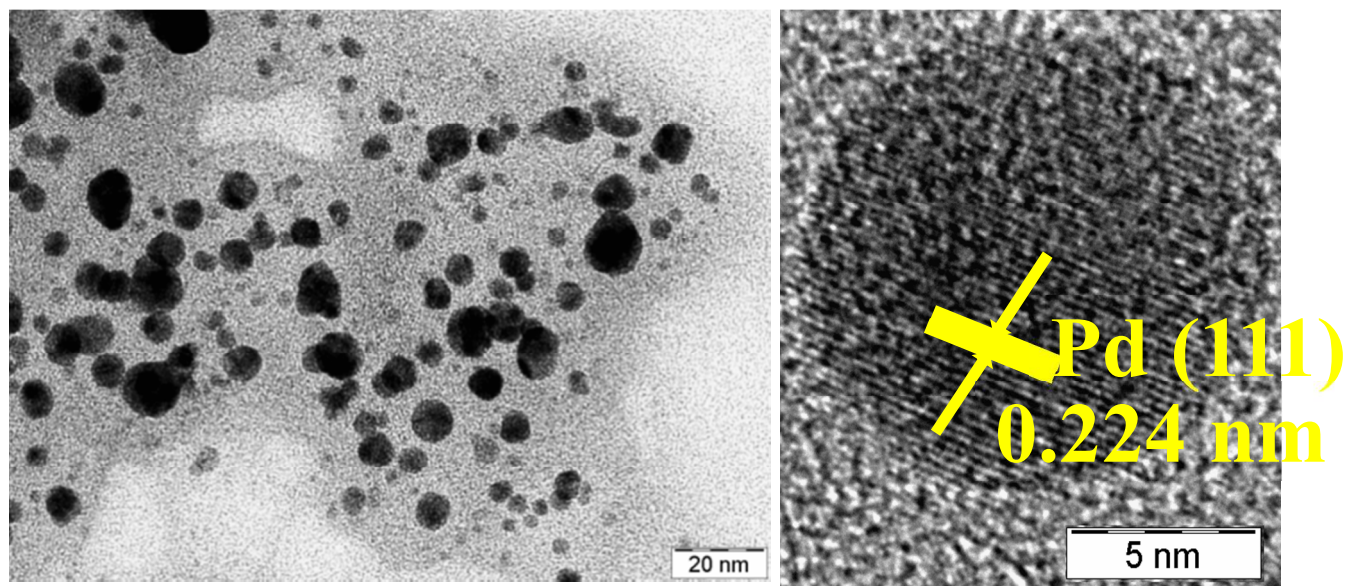
Conditions for the reaction:

(i)  $\text{Br}_2$ , 30% Oleum,  $140^\circ\text{C}$ , 24h (yield 81%); (ii) 4-Cyanophenyl boronic acid,  $\text{Pd}(\text{PPh}_3)_4$ ,  $\text{K}_2\text{CO}_3$ , 1,4-dioxane, DMF,  $\text{N}_2$  atmosphere,  $120^\circ\text{C}$ , 3d (yield 62%); (iii) 6M  $\text{H}_2\text{SO}_4$ ,  $120^\circ\text{C}$ , 12h (yield 98%).

**Scheme 1.** Schematic representation showing the steps in the synthesis of the ligand, 4-(1,10-phenanthrolin-6-yl)benzoic acid.

Jana *et al.* **Figure 1.**

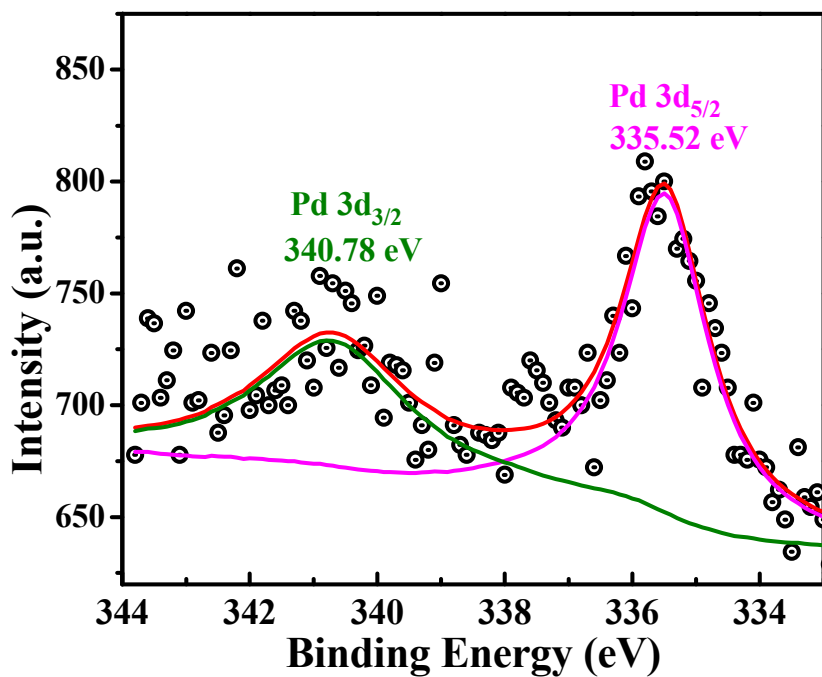




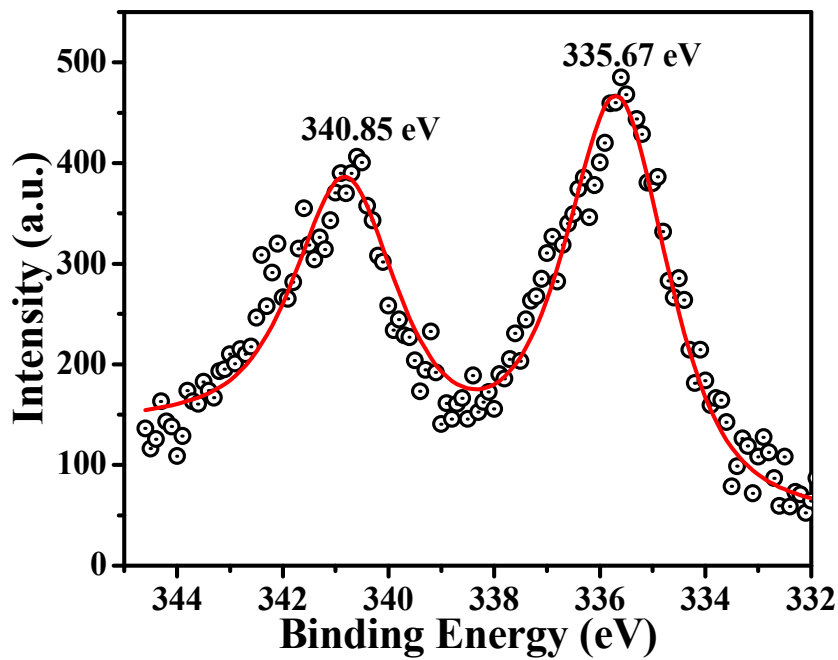
(a)

(b)

Jana *et al.* **Figure 2.**

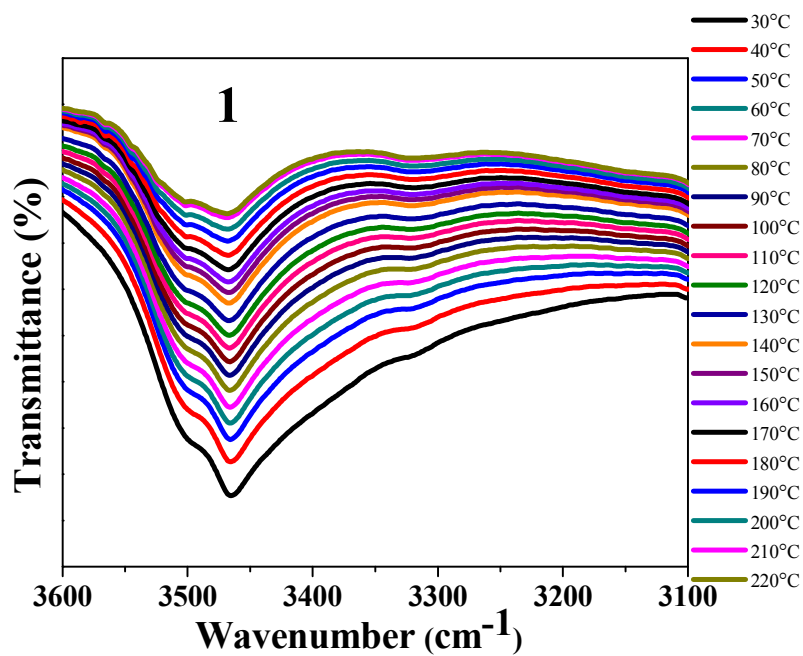


(a)

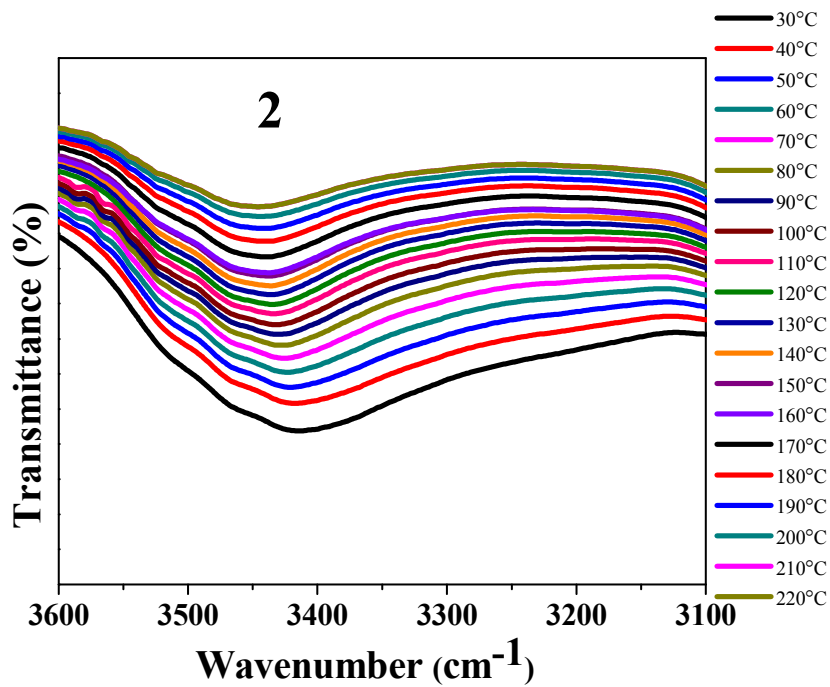


(b)

Jana *et al.* Figure 3.

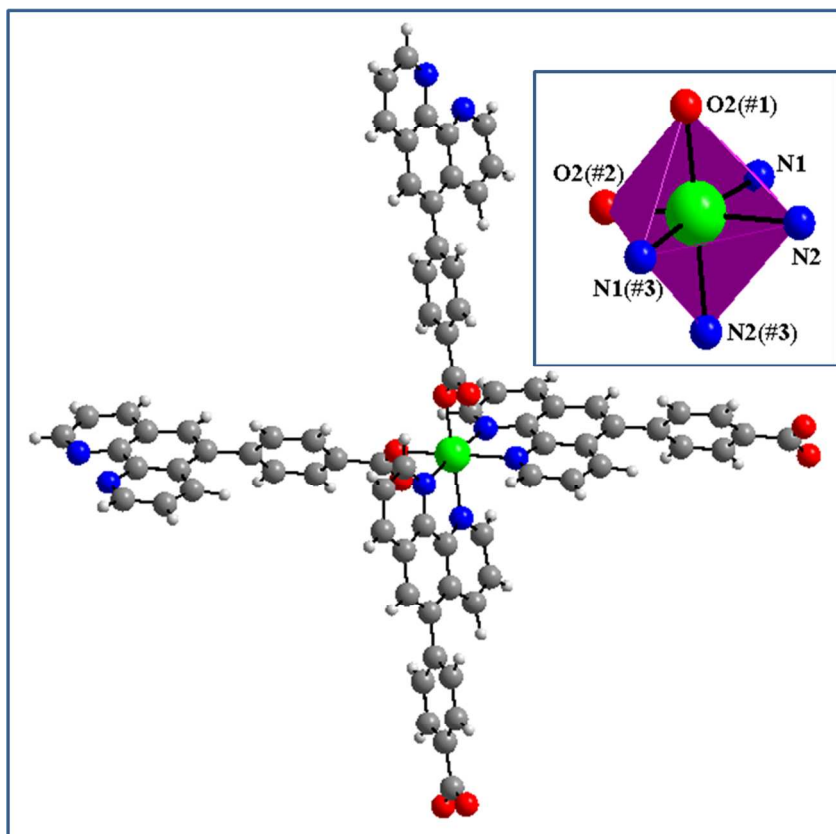


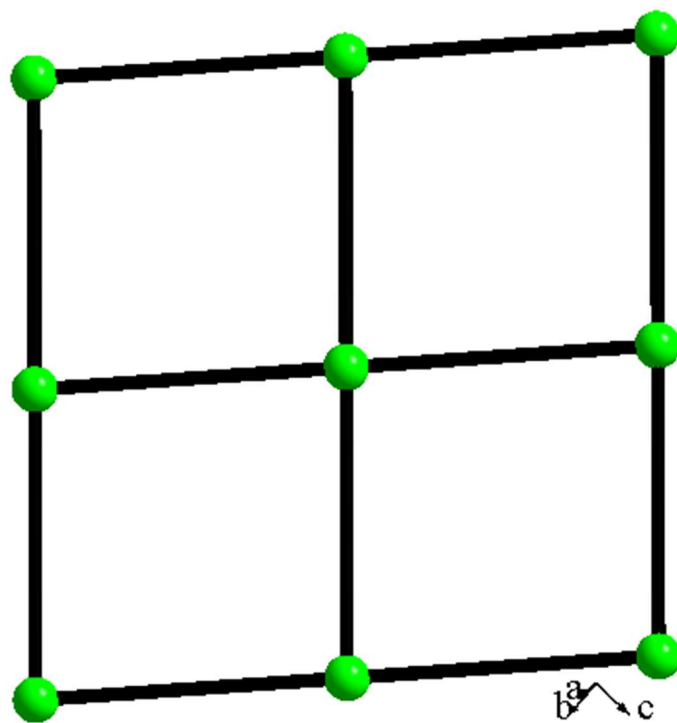
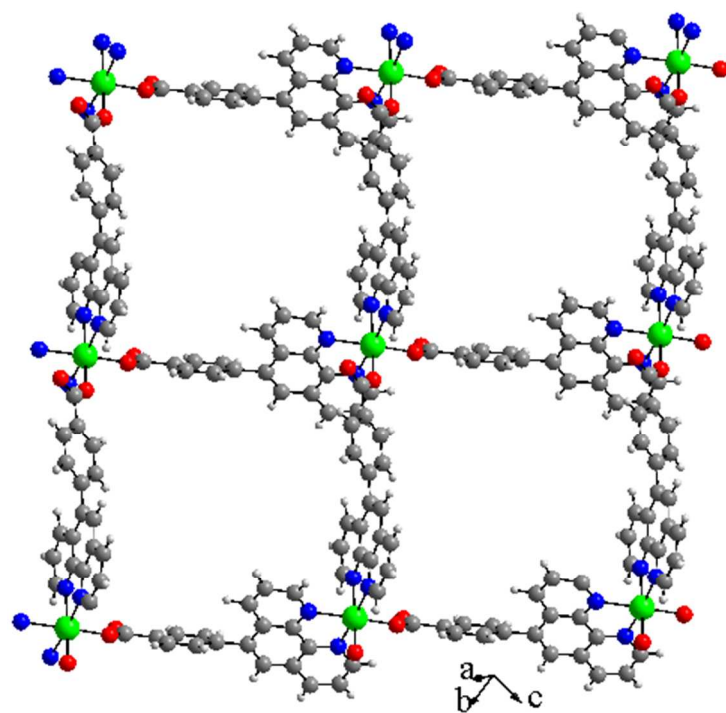
(a)



(b)

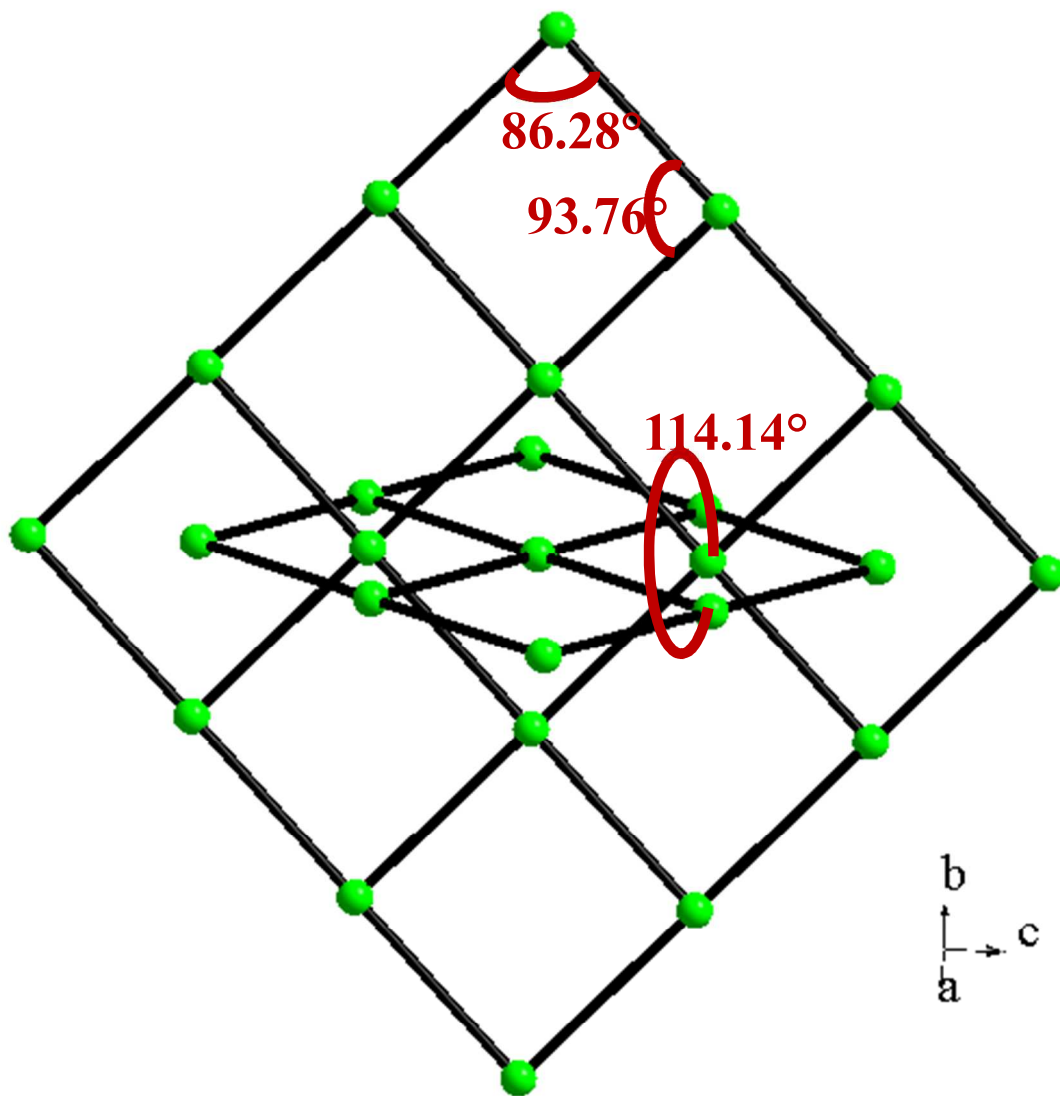
Jana *et al.* Figure 4.

Jana *et al.* Figure 5.

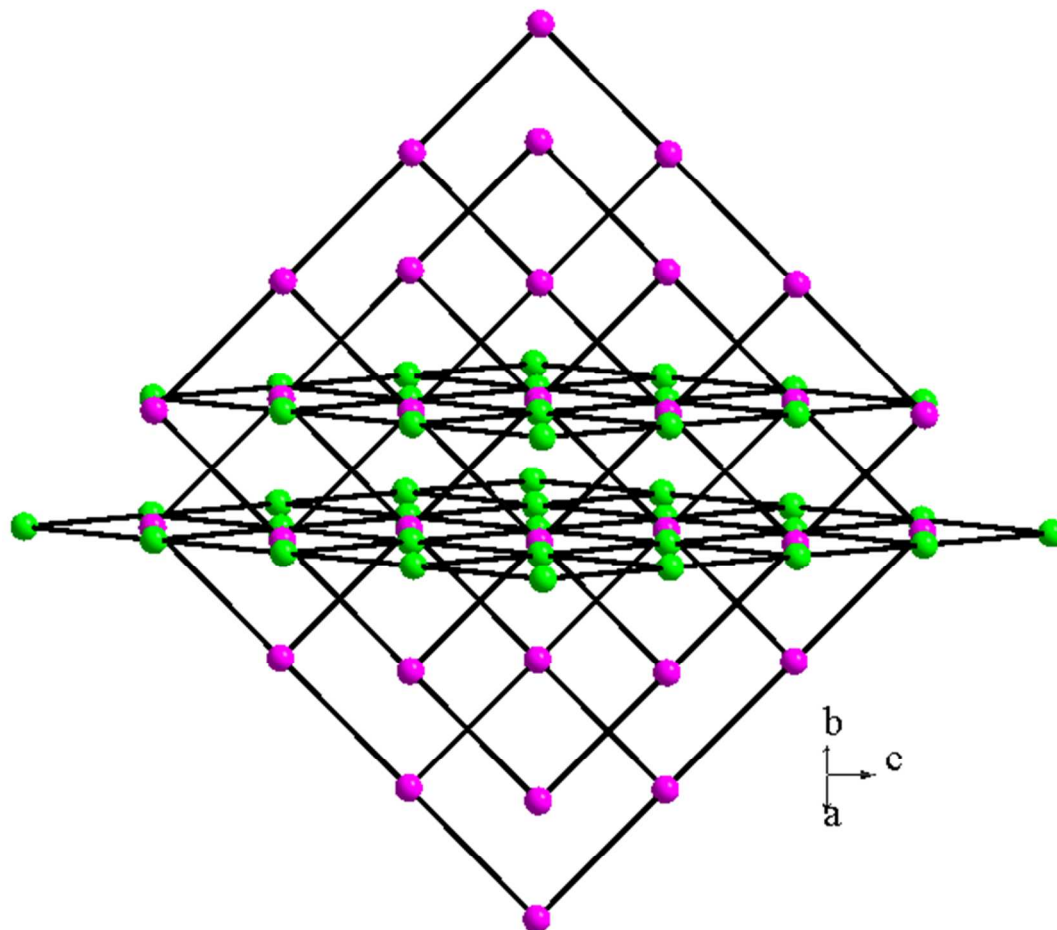


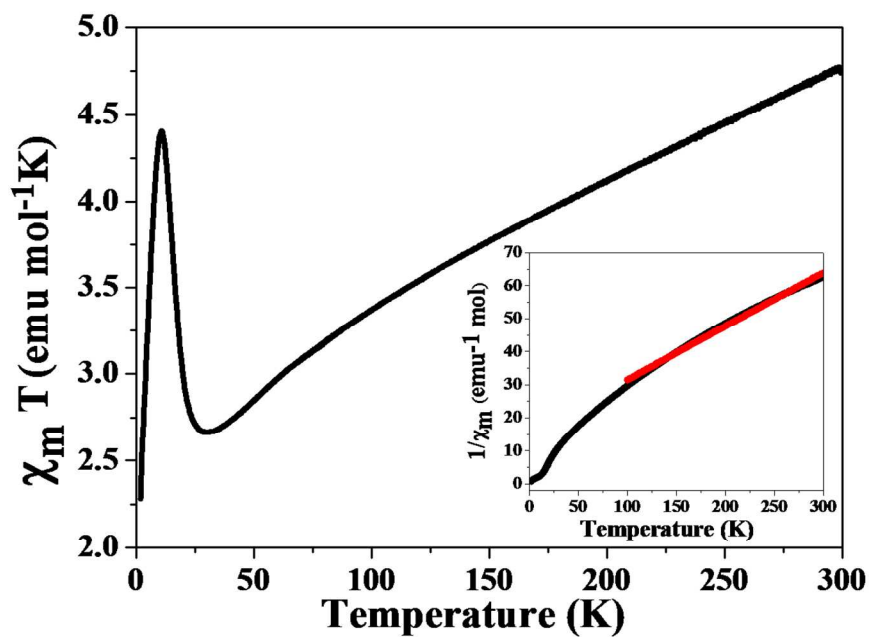
56  
57  
58  
59  
60

Jana *et al.* Figure 6.

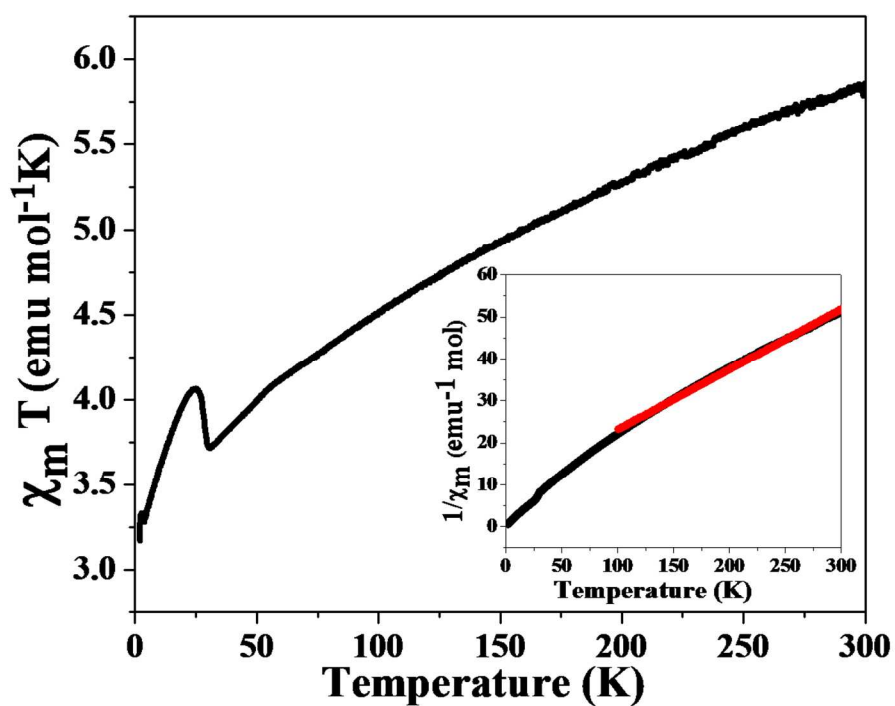


Jana *et al.* Figure 7.

Jana *et al.* **Figure 8.**



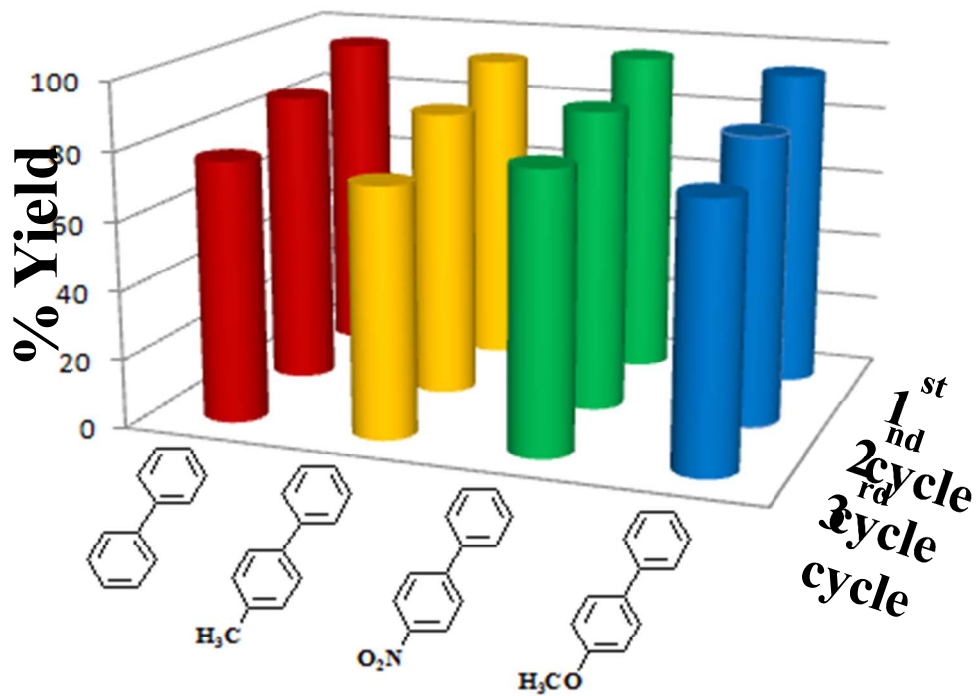
(a)

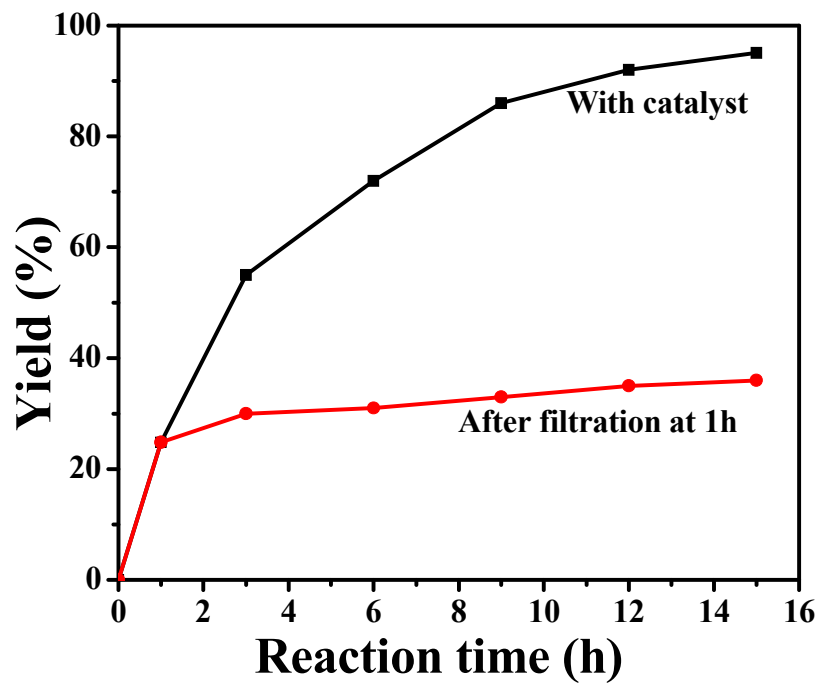


(b)

Jana *et al.* Figure 9.



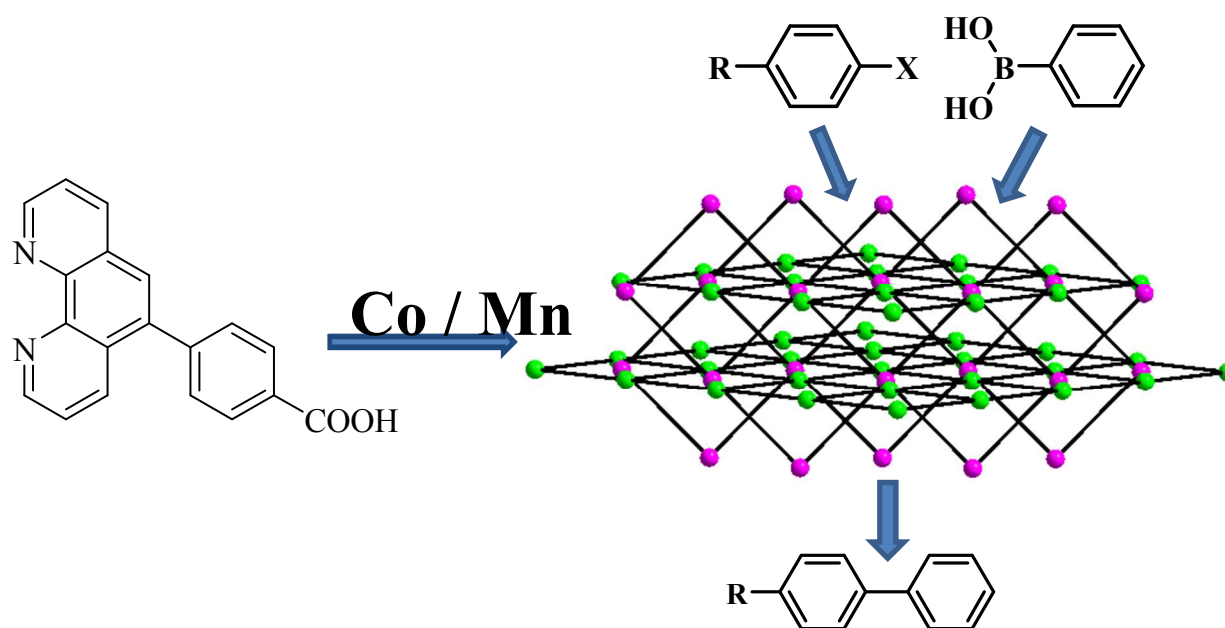
Jana *et al.* Figure 10.

Jana *et al.* Figure 11.

For Table of Contents Use Only

Palladium Nanoparticles Encapsulated in  $[M(C_{19}H_{11}N_2O_2)_2 \cdot H_2O]$  ( $M = Co$  and  $Mn$ ) as a Potential Catalyst for the Homo Coupling of Aryl Halides

Ajay Kumar Jana, Raghunandan Hota and Srinivasan Natarajan\*



A new ligand, 4-(1,10-phenanthroline-6-yl)benzoic acid, on reaction with Co and Mn salts forms a 2-fold interpenetrated structure. Palladium nanoparticles, encapsulated in the compounds, exhibit good catalytic activity for homo-coupling of aryl halides.